Ion-Acoustic Wave Radiation from a Point Source in a Streaming Magnetoplasma

M. Čerček and R. Tavzes

J. Stefan Insitute, E. Kardelj University of Ljubljana, Ljubljana, Yugoslavia

Z. Naturforsch. **38 a**, 608–615 (1983); received January 20, 1983

We report theoretical and experimental results on the radiation pattern of the ion acoustic waves below the ion cyclotron frequency from a small probe in a streaming magnetoplasma. In the fluid approximation with cold ions the ion acoustic resonance cones are found to be drastically changed. Experimental ray velocities and constant phase surfaces are in good agreement with the theoretical results.

1. Introduction

In the past years there has been a considerable interest in radiation phenomena of ion acoustic and electrostatic ion cyclotron waves in a stationary magnetoplasma. Already in 1974 Kuehl [1] theoretically showed that the potential of an oscillating point charge, for frequencies below the ion cyclotron frequency, contains a new resonance cone due to the ion acoustic wave. In a theoretical paper Burrell [2] showed that these new ion acoustic resonance cones occure for frequencies $0 \leqq \omega \leqq \min(\omega_{pi}, \omega_{ci})$ and $\max(\omega_{pi}, \omega_{ci}) \leqq \omega \leqq \omega_{lh}$. The interference structure associated with these cones is sensitive to the ion temperature and could be used for ion temperature measurements in plasmas that meet the conditions of his theoretical derivation: $T_i/T_e \ll 1$ and $\omega_{ci} \gg \omega_{pi}$. Experimentally ion acoustic resonance cones were first observed by Ohnuma et al. [3]. The observed cones were in quantitative accord with theoretical results which include the effect of ion temperature. Simultaneously Belan [4] theoretically and experimentally showed that the resonance cones are asymptotes of hyperbolic constant phase surfaces of ion acoustic waves. Above ω_{ci} the surfaces transform into ellipses which are related to the electrostatic ion cyclotron waves and ion acoustic waves. Ohnuma [5] also measured ray velocities of ion waves near the ion cyclotron frequency. They were found to be restricted to a fixed cone angle which corresponds to the low frequency resonance cone angle.

Reprint requests to M. Čerček, J. Stefan Insitute, Jamova 39, 61000 Ljubljana, Yugoslavia.

It was already shown, theoretically [6–8] and experimentally [9, 10], that the electron drift causes pronounced changes in the properties of high frequency resonance cones. It is the purpose of this paper to investigate the properties of the ion acoustic resonance cone in a streaming plasma.

In Sect. 2 we give the theoretical analysis in the fluid approximation, in Sect. 3 we describe the experimental set up and in Sect. 4 we present experimental results. In Sect. 5 we discuss these results and in Sect. 6 make some conclusions.

2. Theoretical Analysis

We consider a small exciter probe with a charge distribution $q_{ex} = q \exp(-i\omega t)\,\delta(\boldsymbol{r})$ in a streaming magnetoplasma. The plasma flows with a velocity $\boldsymbol{V}_d (= v_d/c_s)$ along the magnetic field $\boldsymbol{B}_0 = B_0 z$. In the electrostatic approximation the potential of the probe can be deduced from the fluid and Poisson equation and is given by

$$\Phi(\boldsymbol{R}, t) = \frac{q\, e^{-\omega t}\, R}{(2\pi)^3 \varepsilon_0 r} \int_{-\infty}^{+\infty} \frac{\varrho_{ex}(\boldsymbol{K})\, e^{i\boldsymbol{K}\cdot\boldsymbol{R}}}{D(\boldsymbol{K})}\, \mathrm{d}\boldsymbol{K}\,, \qquad (1)$$

where $\varrho_{ex}(\boldsymbol{K}) = 1$ for a point charge, $\boldsymbol{K}$ and $\boldsymbol{R}$ are the normalized wave number vector and the observational vector, respectively, and ε_0 is the dielectric constant in vacuum. Both vectors are normalized by $R_L = c_s/\omega_{ci}$ as

$$K = k R_L\,, \qquad R = r/R_L\,, \qquad (2)$$

where $c_s = (\varkappa T_e/m_i)^{1/2}$ is ion acoustic velocity, $\varkappa$ is Boltzmann's constant and T_e and m_i are the electron temperature and the ion mass, respectively. In (1)

0340-4811 / 83 / 0600-0608 $ 01.3 0/0. – Please order a reprint rather than making your own copy.

and in the following calculation we make use of the cylindrical symmetry about the magnetic field B_0:

$$K_\perp = K \sin \Phi\,, \quad K_z = K \cos \Phi\,,$$
$$\varrho = R \sin \Theta\,, \quad Z = R \cos \Theta\,. \tag{3}$$

The dispersion function $D(\boldsymbol{K})$ can be expressed in the fluid approximation with $T = T_e/T_i \gg 1$ as

$$D(K_\perp, K_z) = K_z^2 \left[1 - \frac{\Omega_{pi}^2}{(\Omega - K_z V_d)^2}\right] + K_\perp^2 \left[1 - \frac{\Omega_{pi}^2}{(\Omega - K_z V_d)^2 - 1}\right] + K_{De}^2\,, \tag{4}$$

where $\Omega = \omega/\omega_{ci}$ is the normalized frequency, $\Omega_{pi} = \omega_{pi}/\omega_{ci}$ the normalized ion plasma frequency and $K_{De}^2 = n_0 e^2 R_L^2/\varepsilon_0 \varkappa T_e$ the normalized electron Debye wave number.

After integration of (1) with respect to the azimuthal angle the potential is given by

$$\Phi(\varrho, Z, t) = \frac{q e^{-i\omega t} R}{4\pi^2 \varepsilon_0 r} \cdot \int_{-\infty}^{\infty} e^{iK_z Z} \int_0^{\infty} \frac{J_0(K_\perp \varrho)}{D(K_\perp, K_z)} K_\perp \mathrm{d}K_\perp \mathrm{d}K_z\,. \tag{5}$$

The integral over $K_\perp$ can be evaluated explicitly by using the residue theorem,

$$\Phi(\varrho, Z, t) = \frac{i q e^{-i\omega t} R}{8\pi \varepsilon_0 r} \cdot \int_{-\infty}^{\infty} e^{iK_z Z} \frac{H_0^{(1)}[K_\perp(K_z)\varrho]}{D'(K_z)} \mathrm{d}K_z\,. \tag{6}$$

In (6) $H_0^{(1)}$ is the zeroth-order Hankel function of the first kind and $D'(K_z)$ is given by

$$D'(K_z) = \left(\frac{\partial D}{\partial K_\perp^2}\right)_{D(K_\perp, K_z) = 0} \tag{7}$$

The pole of the integrand is given by the ion acoustic root of the dispersion relation

$$D(K_\perp, K_z) = 0\,. \tag{8}$$

It is shown in Fig. 1 for $V_d = 0$ and $V_d = 0.2$. We introduce a spherical coordinate system (R, Θ, Z), and by keeping the coordinates R and Θ sufficiently large we replace the Hankel function by its asymptotic expansion. Equation (7) can be rewritten as

$$\Phi(R, \Theta, t) = \frac{q\, i \exp\{-i(\omega t + \pi/4)\}\, R}{4\pi \varepsilon_0 \sqrt{2\pi R \sin \Theta}\, r} \cdot \int_{-\infty}^{\infty} \frac{\exp\{i R\, Q(K_z, \Theta)\}}{D'(K_z)\, K_\perp^{1/2}(K_z)} \mathrm{d}K_z\,, \tag{9}$$

where

$$Q(K_z, \Theta) = K_\perp(K_z) \sin \Theta + K_z \cos \Theta\,. \tag{10}$$

We now have an integral that is in the stationary phase form [11], as long as $D'(K_z)^{-1} K^{-1/2}(K_z)$ can be considered slowly varying. The main contribution to the integral comes from small regions near the stationary points given by

$$(\mathrm{d}K_\perp(K_z)/\mathrm{d}K_z) \sin \Theta + \cos \Theta = 0\,. \tag{11}$$

The solutions $K_{zs} = K_{zs}(\Theta)$ of (11) are plotted in Fig. 2 for $V_d = 0$ and $V_d = 0.2$.

If all the stationary points are distinct, the asymptotic expansion of (9) is

$$\Phi(R, \Theta, t) = \frac{q\, i \exp\{-i(\omega t + \pi/4)\}}{4\pi \varepsilon_0 \sin^{1/2}\Theta\, R R_\perp} \cdot \sum_s \frac{\exp\{i R\, Q(K_{zs}, \Theta)\}}{|Q''(K_{zs}, \Theta)|^{1/2} K_\perp^{1/2} D'(K_{zs})}\,, \tag{12}$$

where

$$Q'' = \frac{\mathrm{d}^2 Q}{\mathrm{d}K_z^2} = \frac{\mathrm{d}^2 K_\perp}{\mathrm{d}K_z^2} \sin \Theta\,.$$

If two stationary points are coalescing or, in other words, if $Q'' = 0$ for a given angle Θ, the asymptotic expansion of the integral (9) must be modified. Inspection of the dispersion curve on Fig. 1 shows that there is an inflection point for $V_d = 0.2$ at $\Theta = \Theta_{cd+}$ (marked by an arrow), and from Fig. 2 we see two stationary points coalescing at $\Theta = \Theta_{cd+}$, i.e. in the downstream direction. An asymptotic expansion in such a case was investigated by Chester et al. [11]. It may be shown that the result is given by

$$\Phi(R, \Theta, t) = \frac{-q \exp\{-i(\omega t + \pi/4)\} \sqrt{\pi}}{4\pi \varepsilon_0 (R R_L)^{5/6} \sin \Theta} \cdot \left[\frac{(-\xi^{1/2})^{1/2}}{D'(K_{z1})(K_{\perp 1} K''_{\perp 1})^{1/2}} + \frac{\xi^{1/4}}{D'(K_{z2})(K_{\perp 2} K''_{\perp 2})^{1/2}}\right] \cdot e^{iRa}\, \mathrm{Ai}(R^{2/3}\xi)\,, \tag{13}$$

where

$$\xi = (\tfrac{3}{4})^{2/3}[i \cos\Theta (K_{z2} - K_{z1}) + i \sin\Theta (K_{\perp 2} - K_{\perp 1})]^{2/3},$$
$$a = \tfrac{1}{2}[i \cos\Theta (K_{z1} + K_{z2}) + i \sin\Theta (K_{\perp 1} + K_{\perp 2})]\,.$$

The Airy function behaviour revealed in (13) means that there is a spatial interference pattern associated with the ion acoustic resonance cone in a streaming plasma and in the cold ion approximation, analogous to the one associated with the drift modified

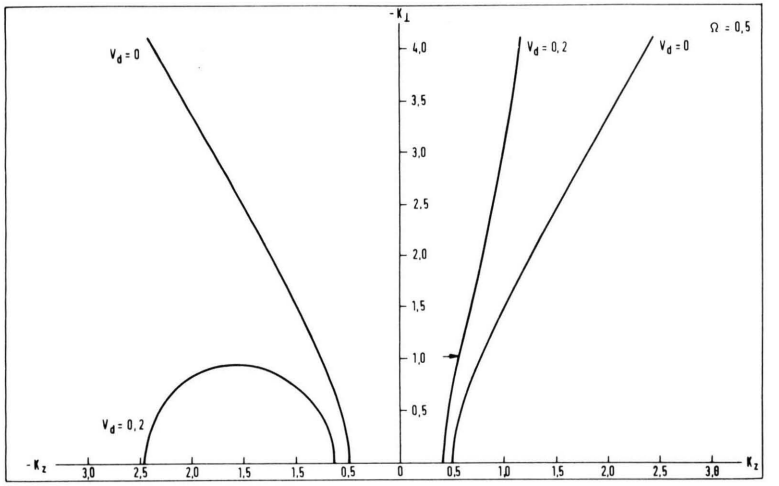

Fig. 1. Dispersion relation $K_\perp$ versus K_z, (8), for $\Omega = 0.5$, $\Omega_{pi} = 5$, $V_d = 0$ and $V_d = 0.2$.

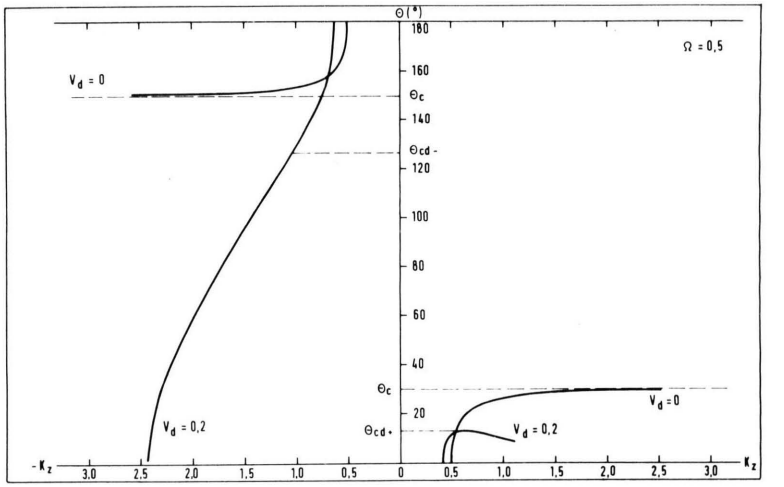

Fig. 2. Stationary points $K_{zs} = K_{zs}(\Theta)$ plot for $\Omega = 0.5$, $V_d = 0$, and $V_d = 0.2$.

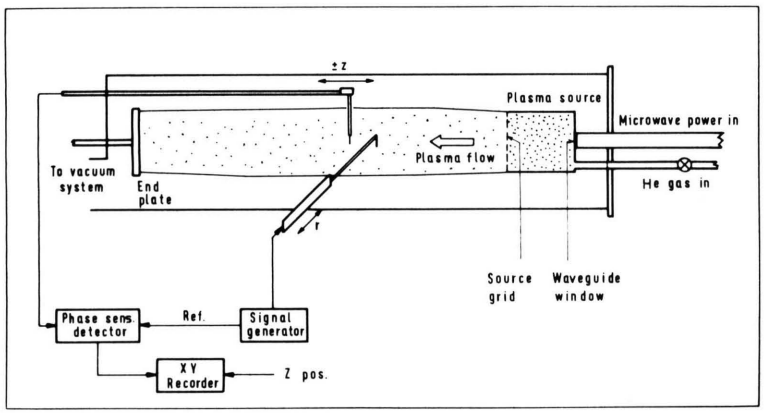

Fig. 6. Scheme of the experimental set up.

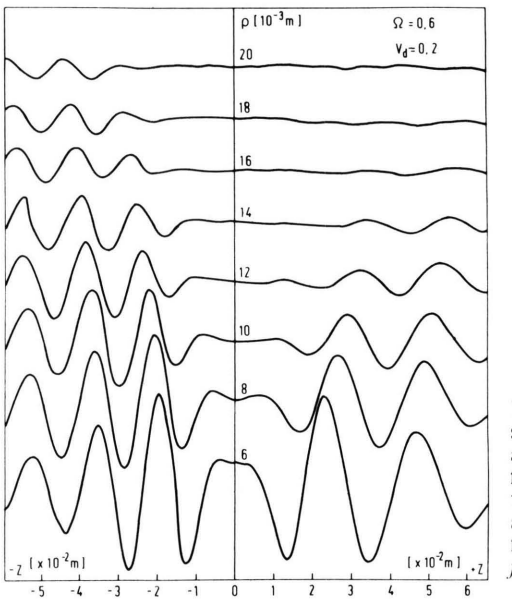

Fig. 7. Interferometric signals in the upstream and downstream direction for several radial distances between the exciter and detector probe. Wave frequency $f = 400$ kHz, $f_{ci} = 665$ kHz, $V_d = 0.2$.

cold plasma resonance cone [8]. The angle of the maximum potential Θ'_{cd+} is a little smaller than Θ_{cd+} but very much smaller than the cold resonance cone angle $\Theta_c = \arcsin \Omega$ in a stationary plasma. For angles Θ near $\pi - \Theta_c$ in the upstream direction the inspection of (12) shows that the amplitude of the wave potential has a maximum at an angle $\Theta_{cd-} > \Theta'_{cd-} > \Theta_c$ (Figure 10).

The stationary points given by (11) should give together with the dispersion relation (8) the magnitude and the direction of the wavenumber vector $\boldsymbol{K}(K, \Phi)$ at an observation point $\boldsymbol{R}(R, \Theta)$. By using the relations (3), (11) can be written as

$$\operatorname{tg}(\Theta - \Phi) = -\frac{1}{K}\frac{\partial K}{\partial \Phi} = \operatorname{tg} \alpha\,. \tag{14}$$

This is the equation which describes the relation between the directions of the group and phase velocities [12]. The group velocity vector $\boldsymbol{V}_g(V_g, \Theta)$ is in our problem therefore directed radialy outward. It is therefore very useful to investigate the group, phase and ray velocities which can be determined from the dispersion relation. From the latter the constant phase surfaces can be deduced, which can be directly compared with the experiment.

The magnitude of the group velocity can be expressed in terms of $D(K_\perp, K_z)$ as

$$V_g = \left[\left(\frac{\partial D}{\partial K_\perp}\Big/\frac{\partial D}{\partial \Omega}\right)^2 + \left(\frac{\partial D}{\partial K_z}\Big/\frac{\partial D}{\partial \Omega}\right)^2\right]^{1/2}, \tag{15}$$

and its direction as

$$\operatorname{ctg} \Theta = \frac{\partial K_\perp}{\partial K_z} = \frac{\partial D}{\partial K_z}\Big/\frac{\partial D}{\partial K_\perp}\,. \tag{16}$$

The phase velocity is given by

$$V_p = (\Omega/K_z)\cos \Phi \tag{17}$$

and the ray velocity, being the phase velocity in the direction of the group velocity, by

$$V_r = (\Omega/K)\ 1/\cos \alpha\,. \tag{18}$$

The equation of constant phase surface is obtained from

$$R = (\omega t - C)/K \cos \alpha\,, \tag{19}$$

where C is a constant.

Using (15) to (19) we have constructed phase, group and ray velocity polar plots as given on Figs. 3, 4 and 5. Figure 3 was plotted for a stationary plasma to facilitate the comparison with the results

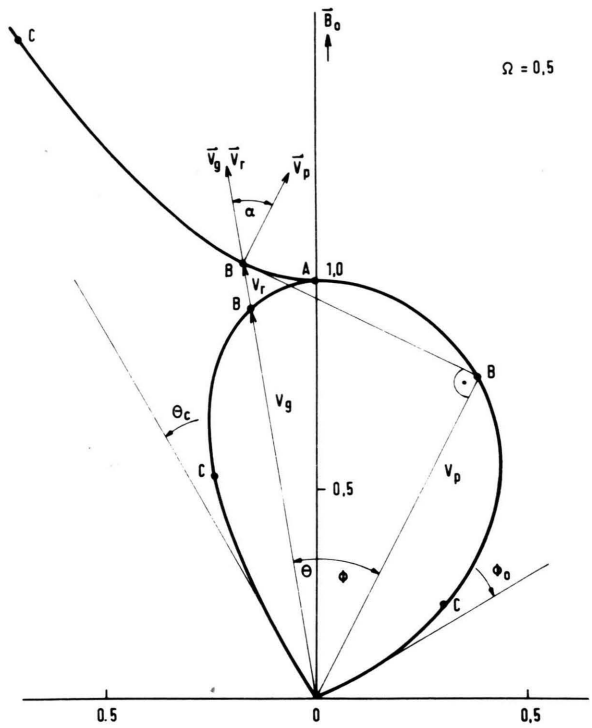

Fig. 3. Normalized phase velocity V_p (right side), group velocity V_g and ray velocity V_r (left side) plot versus the angle to the magnetic field in a stationary plasma. The marks on the phase velocity curve correspond to those on the group and ray velocity curves.

in the streaming plasma. The phase velocity is real only for angles $\Phi \leqq \Phi_0 = \arccos \Omega$. The angle Φ_0 is the phase velocity resonance cone angle. The group velocity is real only for angles $\Theta \leqq \Theta_c$, the group velocity resonance cone angle. The ray velocity V_r tends to infinity at $\Theta = \Theta_c$.

In the streaming plasma the situation is drastically changed. In the downstream direction, Fig. 4, the phase velocity is real for all angles $0 \leqq \Phi \leqq \pi/2$ and there is no phase velocity resonance cone angle. The group velocity resonance cone angle Θ_{cd+} still exists, but is smaller than the resonance cone angle Θ_c in the stationary plasma. The most interesting aspect of this figure is the double valued group velocity for $\Theta < \Theta_{cd+}$. The double value of the group velocity arises from the fact that two phase velocities pointing in two different directions can have their corresponding group velocities pointing in one and the same direction. The two values of the group velocity correspond to two propagating waves forming the interference structure given by (13). The ray velocity

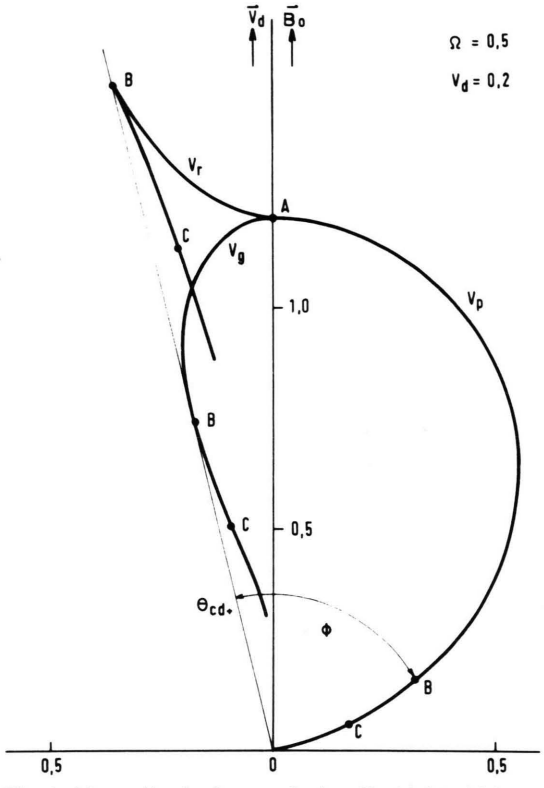

Fig. 4. Normalized phase velocity V_P (right side), group velocity V_g and ray velocity V_r (left side) plot versus the angle to the magnetic field in the downstream direction for $\Omega = 0.5$ and $V_d = 0.2$. The marks on the V_p curve correspond to those on the group and ray velocity curves.

is finite on the resonance cone and is also double valued inside it.

In the upstream direction, Fig. 5, the phase velocity is real only for angles Φ_d and is double valued. The group velocity is single valued and real for all angles $\pi \geqq \Theta \geqq 0$. For angles $\Theta \leqq \pi/2$ the axial components of the group velocity and phase velocity are antiparallel, so there is a new backward wave in the downstream plasma. The ray velocity retains its hyperbolic form for angles $\Theta \leqq \pi - \Theta_{cd-}$ and is single valued for all angles Θ.

Finally we should point out that there should appear a new interference structure for angles $\Theta_{cd+} \leqq \Theta \leqq \pi - \Theta_{cd-}$, analogous to the interference structure associated with the high frequency resonance cone in a drifting plasma [7, 8]. This new interference pattern arises due to the interference of the new wave for $\Theta < \pi - \Theta_{cd-}$ with the nonpropagating potential outside the downstream resonance cone. As can be seen from the ray velocity plot, the phase of the wave in that range varies very fast with the angle Θ giving the interference structure.

3. Experimental setup

The experiment was performed in an ECR plasma device shown schematically on Figure 6. The stainless steel vacuum chamber with the plasma source is situated in a dc magnetic field, uniform in the experimental region. The plasma source is an open ended circular waveguide which continuously couples microwave power (10 W, 9.3 GHz) into the plasma at ECR. The source grid separates the experimental region from the source region and improves the quiescence and homogeneity of the plasma column. Helium gas is continuously leaked through the system and the pressure is precisely

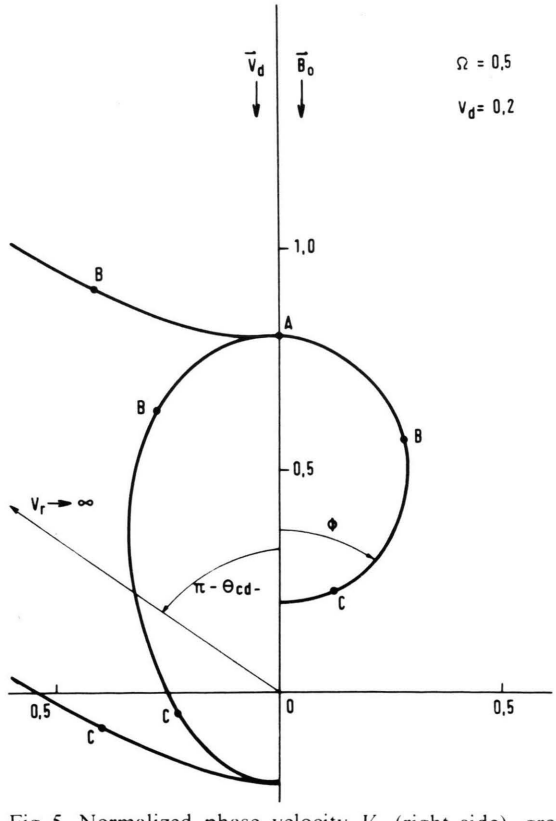

Fig. 5. Normalized phase velocity V_p (right side), group velocity V_g and ray velocity V_r (left side) plot in polar coordinates in the upstream direction for $\Omega = 0.5$ and $V_d = 0.2$. The marks on the V_p curve correspond to those on the group and ray velocity curves.

controled by a needle valve. In the experimental region the magnetic field is decreased to a uniform value of 0.17 T and the plasma forms a column of $7 \cdot 10^{-2}$ m in diameter and 0.50 m long. The plasma density is about $2 \cdot 10^{15}\,\mathrm{m}^{-3}$ and the electron temperature is 2–3 eV. Both parameters were obtained by a Langmuir probe. The exciting and detecting tungsten wire probes ($d = 1.15 \cdot 10^{-4}$ m, $l = 4 \cdot 10^{-3}$ m) are movable along and perpendicular to the magnetic field. We have used $(2-5) \cdot 10^{-3}$ m probe lengths. No dependence of potential pattern on probe length was noted. The potential patterns versus axial distance are displayed on an xy recorder using the interferometer technique.

4. Experimental results

Typical interferometric patterns of the ion acoustic waves are shown in Figure 7. The signals were obtained with an axially movable probe at different radial distances from the perpendicularly movable probe. The ion acoustic wave measured at the radial distance $r = 0$ obeys the simple dispersion relation $\omega = k_z c_s \pm v_d$. The measured phase velocity at $r = 0$ is in good agreement with the ion acoustic velocity $c_s = (\varkappa T_e/m_{He})^{1/2} = 6.4 \cdot 10^3$ m/s with $T_e = 2$ eV measured with the Langmuir probe. The measurements give for the drift velocity $v_d = 1.3 \cdot 10^3$ m/s. All plasma parameters dependend on the working pressure ($10^{-4} - 10^{-3}$ torr).

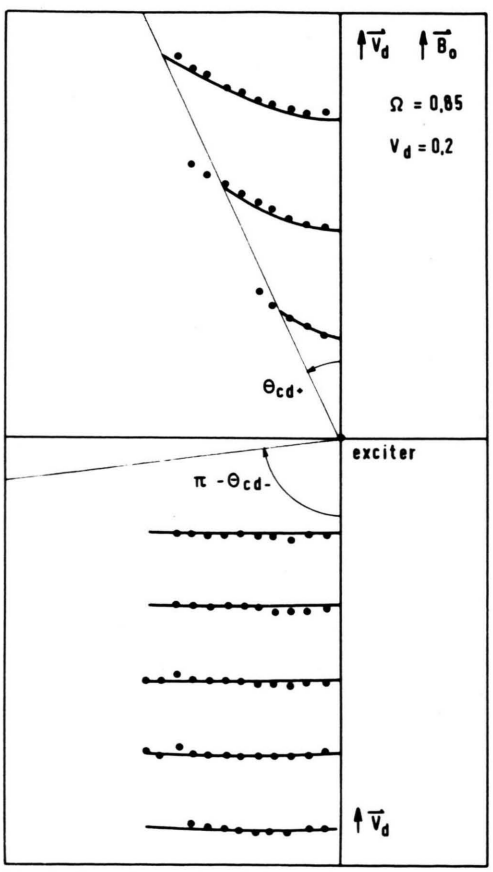

Fig. 8. Experimental and theoretical constant phase curves for $f = 565$ kHz, $f_{ci} = 665$ kHz and $V_d = 0.2$ in the downstream and upstream directions.

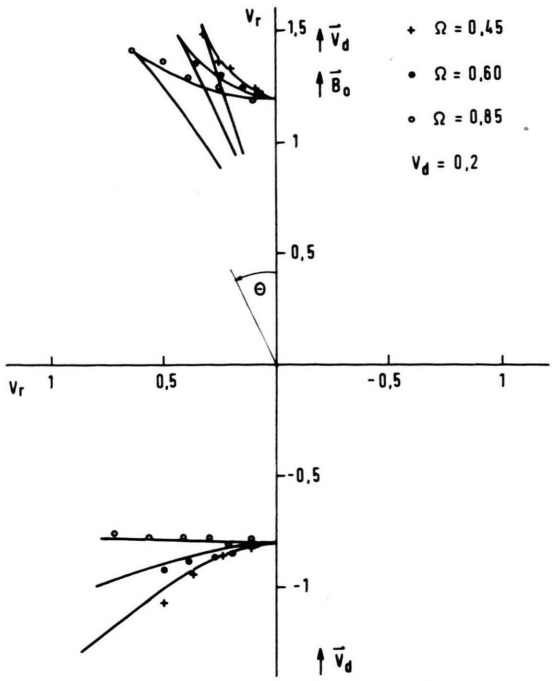

Fig. 9. Experimental and theoretical ray velocities versus the angle Θ for several values of exciter frequency and for $V_d = 0.2$ in the downstream and upstream directions.

In Fig. 8 the wave fronts, which were obtained from the experimental data like those in Fig. 7, are plotted in polar coordinates. The angle Θ is measured from the magnetic field axis z parallel to the drift velocity direction. The plotted wave fronts are in fact constant phase surfaces. They show the well known hyperbolic behaviour for frequencies $\Omega < 1$ but are not symmetric with respect to the source because of the additional anisotropic property of the medium, the stream of the plasma. In Fig. 9 the measured ray velocities are presented for various detection angles with the exciting frequency as the parameter. The measured angular pattern of the

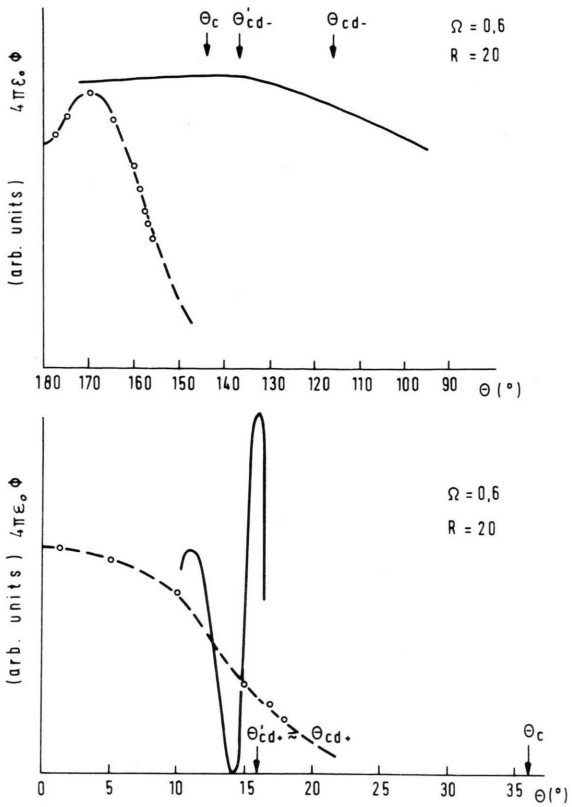

Fig. 10. Experimental and theoretical wave amplitude pattern versus the angle Θ in the upstream and downstream directions for $f = 400$ kHz, $f_{ci} = 665$ kHz and $V_d = 0.2$.

wave amplitude is plotted versus Θ for $\Omega = 0.6$ in Figure 10. In the upstream direction it increases a little at first as the angle Θ increases and then decreases to zero. In the downstream direction it only decreases with the angle Θ.

5. Discussion

In Fig. 8 the closed circles indicate the observed constant phase surfaces and are in good agreement with the theoretical ones obtained from (19), which are shown by the solid lines. The measurements were done with $f = 565$ kHz, $f_{ci} = 665$ kHz, $T_e = 2$ eV and $V_d = 0.2$. However we were not able to measure constant phase surfaces for $K_Z(\Theta) \geqq K_Z(\Theta_{cd+})$ and $-K_Z(\Theta) \geqq -K_Z(\pi - \Theta_{cd-})$ (Figure 2). The solid curves in Fig. 9 are the theoretical ray velocities calculated from (18). The experimentally obtained values are found to be in good agreement with theoretical ones. The results are given for the same plasma parameters as in Figure 8. It is very interesting that the resonance cone shift as measured from ray velocity surfaces is not equal in both directions of the plasma stream. For $V_d = 0.2$ and $\Omega = 0.45$ it is $+\Delta\Theta_{cd-} = 23°$ in the upstream direction and $-\Delta\Theta_{cd+} = 14°$ in the downstream direction. This fact is also confirmed by the experiment.

Next we discuss the wave amplitude versus the angle Θ. In Fig. 10 the theoretical wave amplitude has a maximum in the upstream direction at $\Theta = \pi - \Theta_{cd-}$. Experimentally, the amplitude increases at first to the angle $\Theta = 10°$ $(= \pi - 170°)$ and then decreases to zero at the angle $\Theta = 50°$. In the downstream direction we should obtain, according to the theory, an Airy interference structure with the primary maximum at $\Theta_{cd+} = 16°$. The experimental data only decrease with Θ to zero at $\Theta = 24°$. We notice that the interference structure is totally missing and that there is no wave in the region of $\Theta_{cd+} \leqq \Theta \leqq \pi - \Theta_{cd-}$. In order to get better agreement with experiment we think it is essential to take into account: (a) the results of the investigation of Ohnuma [13] where the amplitude of an ion acoustic wave was greatly enhanced in the direction of the magntic field even though the plasma itself was isotropic. It is possible that the source coupling mechanism is important; (b) Kinetic theory and damping should be applied. The theoretical and experimental results [14, 15] show that the damping of ion acoustic waves in a magnetic field increases with propagation angle. The angular amplitude pattern may be considerably altered when the warm plasma model ($T_i \neq 0$) is used. This might be the aim of a future investigation.

6. Conclusion

In this paper the effect of a field aligned plasma stream on the ion acoustic resonance cone and ray velocity surface in a magnetoplasma has been investigated theoretically and experimentally. The main result of the theoretical investigation in a fluid approximation is that the group velocity resonance cone disappears in the upstream direction of the plasma flow and the downstream group velocity resonance cone angle is smaller than the cone angle in the stationary plasma. The group and ray velocities are double valued in the downstream direction. In the amplitude pattern an interference structure appears for angles $0 \leqq \Theta \leqq \Theta_{cd+}$ and $\Theta_{cd+} < \Theta < \pi - \Theta_{cd-}$.

The experimental results confirm the theoretical predictions for the ray velocity pattern for smaller propagation angles Φ, but for larger values and for the description of amplitude measurements the more adequate kinetic theory with inclusion of collisional wave damping seems to be necessary.

[1] H. H. Kuehl, Phys. Fluids **17,** 1636 (1974).
[2] K. H. Burrell, Phys. Fluids **18,** 897 (1975).
[3] T. Ohnuma, T. Kuwabara, K. Shibata, and S. Adachi, Phys. Rev. Lett. **37,** 205 (1976).
[4] P. Bellan, Phys. Rev. Lett. **37,** 903 (1976).
[5] T. Ohnuma, T. Kuwabara, S. Adachi, and K. Shibata, Phys. Rev. **A 15,** 392 (1977).
[6] H. H. Kuehl, Phys. Fluids **17,** 1275 (1974).
[7] N. Singh, Phys. Fluids **20,** 1692 (1977).
[8] L. R. O. Storey and J. Thiel, Phys. Fluids **21,** 2325 (1978).
[9] K. Lücks and M. Krämer, Plasma Phys. **22,** 879 (1980).
[10] R. W. Boswell and J. Thiel, Phys. Fluids **24,** 2120 (1981).
[11] H. Jeffreys, Asymptotic Approximations, Oxford Univ. Press 1962, Chapter 2.
[12] E. H. Holt and R. E. Haskell, Foundations of Plasma Dynamics, MacMillan Comp. New York 1965, Chapter 13.
[13] T. Ohnuma, H. Izawa, and S. Adachi, Phys. Rev. **12 A,** 1648 (1975).
[14] D. G. Lominadze and K. N. Stepanov, Zh. Tehn. Fiz. **10,** 1823 (1964).
[15] A. Hirose, I. Alexeff, and W. D. Jones, Phys. Fluids **13,** 1290 (1970).